Electronic Supplementary Material (ESI) for RSC Advances.

Supplementary Information for:

Enhancing Li-ion capacity and rate capability in cation-defective vanadium ferrite aerogels via aluminum substitution

Christopher N. Chervin,[1] Ryan H. DeBlock,[2] Joseph F. Parker,[1] Bethany M. Hudak,[3] Nathaniel L. Skeele,[1] Jesse S. Ko,[4] Debra R. Rolison,[1] and Jeffrey W. Long[11]

[1]*Surface Chemistry Branch, Code 6170, U.S. Naval Research Laboratory, Washington, DC 20375, USA*

[2] *NRC Postdoctoral Associate at the Naval Research Laboratory, Washington, DC 20375, USA*

[3] *Materials & Systems Branch, Code 6360, U.S. Naval Research Laboratory, Washington, DC 20375, USA*

[4]*Former NRC Postdoctoral Associate at the Naval Research Laboratory, Washington, DC 20375, USA*

[1] Author to whom correspondence should be addressed. Email: jeffrey.long@nrl.navy.mil

Fig. S1

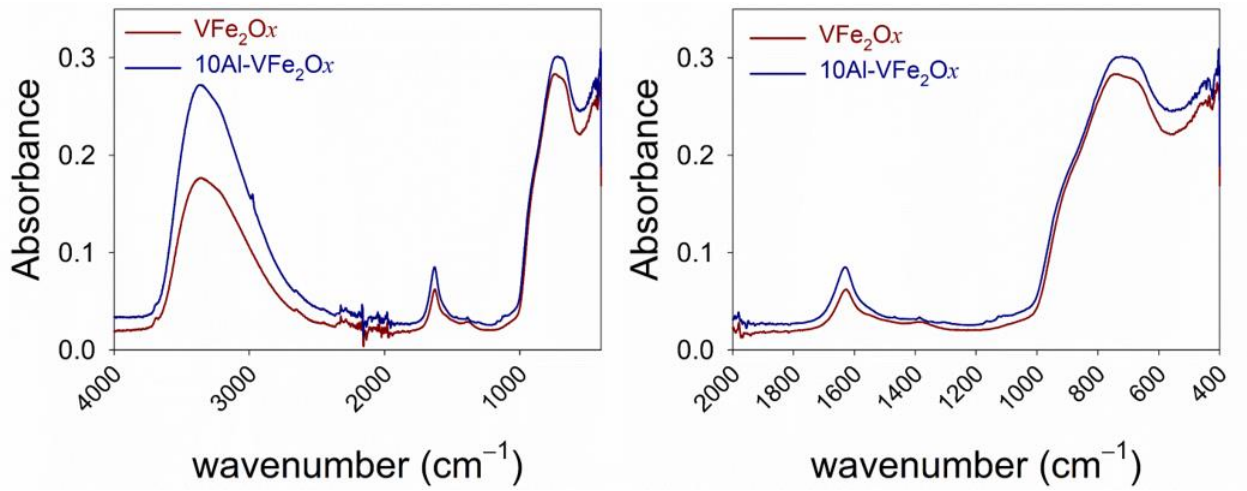

Fig. S1. Attenuated total reflectance infrared spectra of VFe_2Ox and 10Al-VFe_2Ox heated to 300 °C in O_2. Spectra on the left shows the full range and spectra on the right shows the region from 2000 to 400 cm^{-1}.

The spectra include a broad band from 3750 to 3000 cm^{-1}, typical for adsorbed water, expected because the data are collected in ambient conditions where the high surface-area aerogels readily adsorb atmospheric water. The spectra also show a band centered at ~1630 cm^{-1} that correlates with C=O or C=C stretching from residual organic components, a byproduct of the synthesis previously observed in Zr*O*x*H*y-based aerogels prepared by the epoxide-initiated method.

Fig. S2

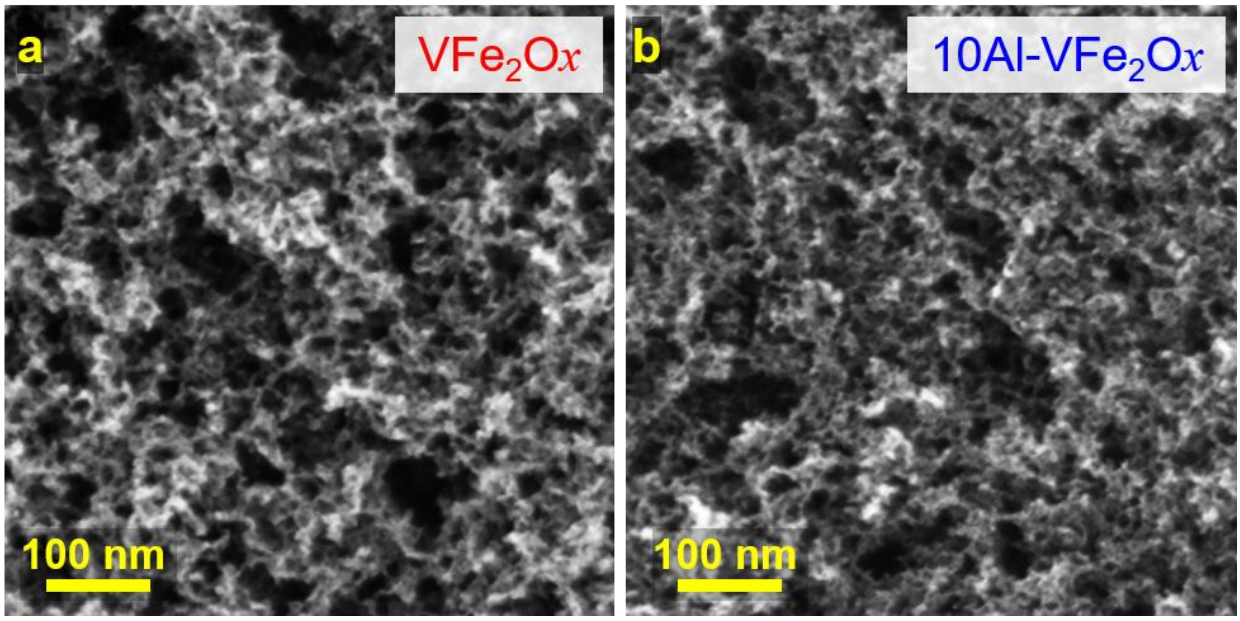

Fig. S2. Scanning electron micrographs of **(a)** VFe_2Ox heated to 300 °C in O_2 and **(b)** 10Al-VFe_2Ox heated to 300 °C in O_2.

Fig. S3

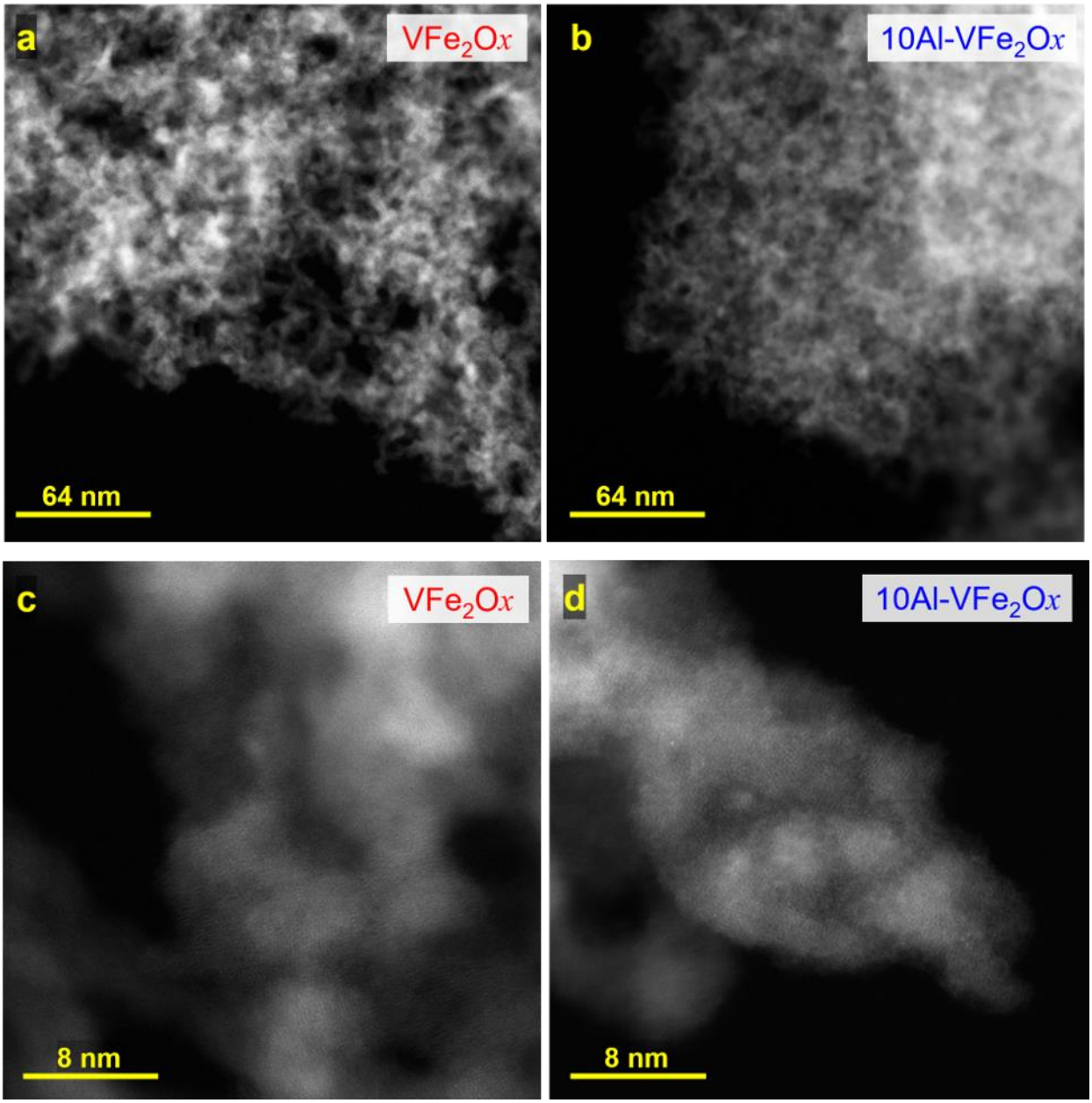

Fig. S3. Transmission electron micrograph of **(a,c)** VFe_2Ox heated to 300°C in O_2 and **(b,d)**10Al-VFe_2Ox heated to 300°C in O_2.

Fig. S4

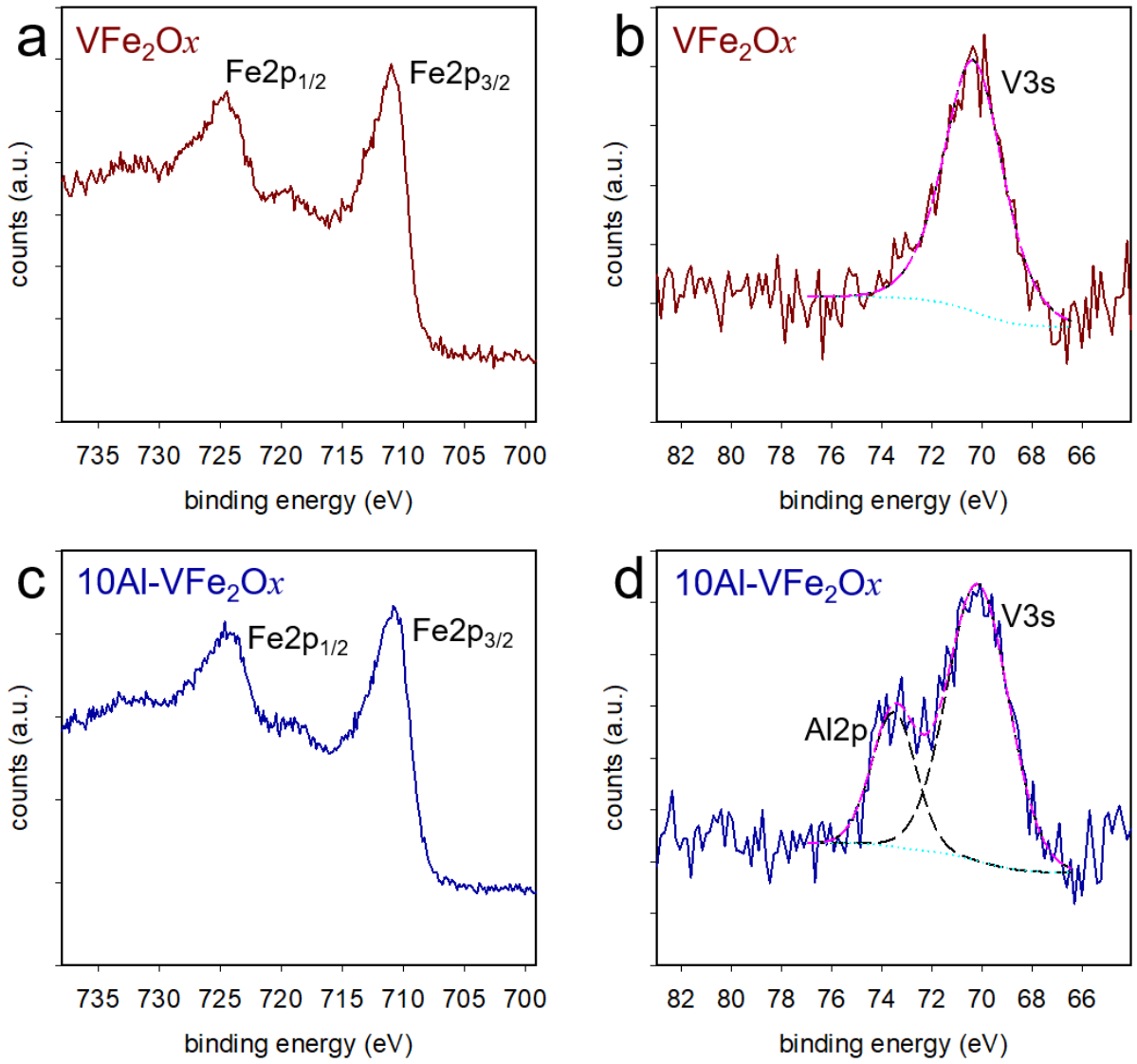

Fig. S4. X-ray photoelectron spectra of VFe_2Ox (a) Fe2p and (b) Al2p/V3s regions; and 10Al-VFe_2Ox (c) Fe2p and (d) Al2p/V3s regions.

Fig. S5

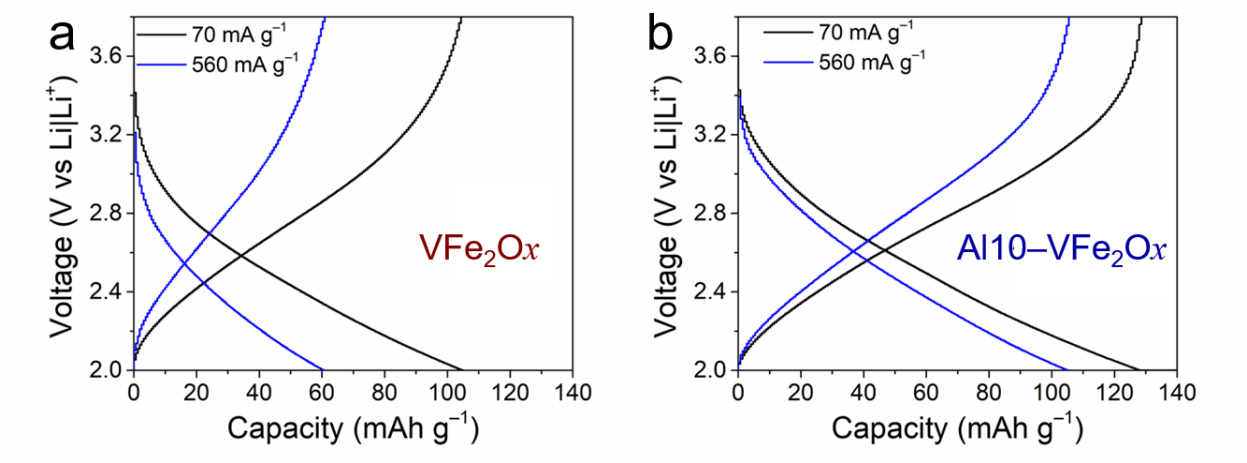

Fig. S5. Galvanostatic charge/discharge testing on both (a) VFe_2Ox and (b) 10Al-VFe_2Ox aerogels at 70 and 560 mA g^{-1} with current density normalized to the mass of active material in the powder-composite electrode

Fig. S6

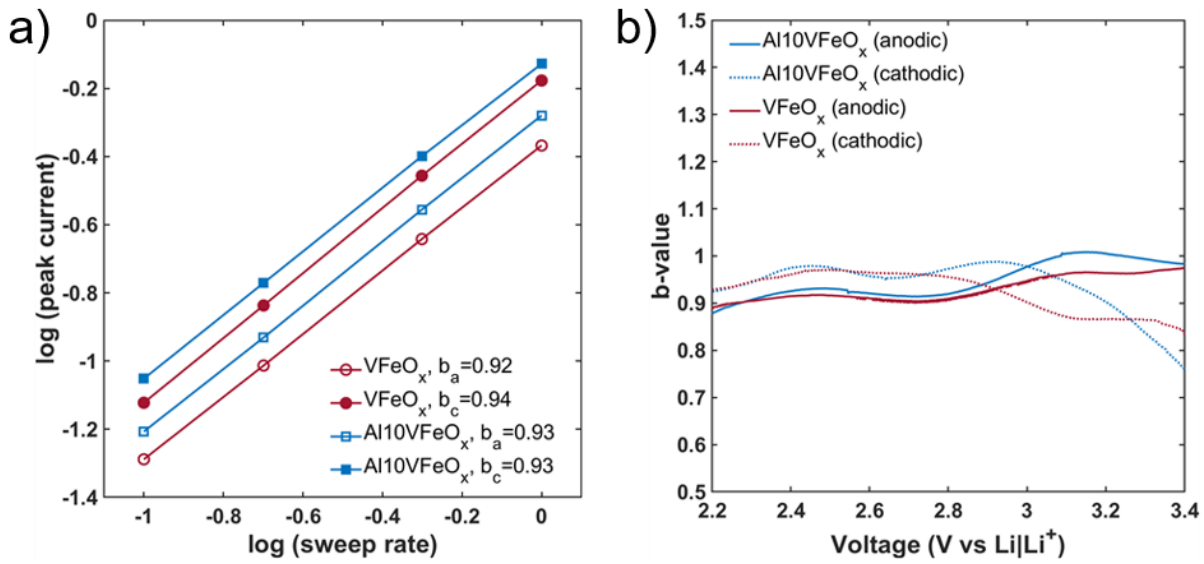

Fig. S6. (a) peak current b-value analysis for V_2FeOx (red) and 10Al-VFeO*x* (blue) with both anodic (open markers) and cathodic (closed markers). Minimum R^2 is 0.9999; (b) Variation in b-as a function of potential. The first and last 200mV removed for polarization discrepancies.

Diffusion analysis was performed by plotting the b-value across the entire potential window scanned. By processing the data in this way, voltammograms can still be fit to Equation 1 accurately in the absence of well-defined redox peaks. Polarization effects disrupt the analysis when changing sweep direction (i.e., switching from a cathodic sweep to an anodic one or vice versa), so the first and last 200 mV are removed from the analysis.

Table S1. Summary of N_2-physisorption and elemental analysis results for VFe_2O_x and 10Al-VFe_2O_x

Sample	BET surface area ($m^2\ g^{-1}$)	BJH adsorption pore volume ($cm^3\ g^{-1}$)	BJH adsorption pore width (nm)	Fe: Al+V (atomic ratio)	% Al on V-site
VFe_2O_x	229	3.4	62	2.2	0
10Al-VFe_2O_x	327	3.7	51	2.0	9.7

Table S2. Summary of galvanostatic charge–discharge first cycle efficiency and fifth cycle hysteresis for VFe_2Ox and 10Al-VFe_2Ox

Sample	First Cycle Efficiency	Hysteresis* 70 mA g^{-1} (V)	Hysteresis* 560 mA g^{-1} (V)	Hysteresis$^{\Delta}$ 70 mA g^{-1} (V)	Hysteresis$^{\Delta}$ 560 mA g^{-1} (V)
VFe_2Ox	85%	0.36	1.1	0.38	0.52
10Al–VFe_2Ox	92%	0.26	0.66	0.30	0.35

*Calculated by dividing the total energy for either charge/discharge by the total capacity for the corresponding charge/discharge to obtain an average potential. Average voltage of discharge was then subtracted from the operating voltage for charge to calculate hysteresis.

$^{\Delta}$Calculated by subtracting the potential at 50% energy upon discharging from the potential at 50% energy upon charging.